Spline Thin-Shell Simulation of Manifold Surfaces

Kexiang Wang, Ying He, Xiaohu Guo, and Hong Qin

Department of Computer Science
Stony Brook University
Stony Brook, NY 11790-4400, USA
{kwang|yhe|xguo|qin}@cs.sunysb.edu

Abstract. It has been technically challenging to effectively model and simulate elastic deformation of spline-based, thin-shell objects of complicated topology. This is primarily because traditional FEM are typically defined upon planar domain, therefore incapable of constructing complicated, smooth spline surfaces without patching/trimming. Moreover, at least C^1 continuity is required for the convergence of FEM solutions in thin-shell simulation. In this paper, we develop a new paradigm which elegantly integrates the thin-shell FEM simulation with geometric design of arbitrary manifold spline surfaces. In particular, we systematically extend the triangular B-spline FEM from planar domains to manifold domains. The deformation is represented as a linear combination of triangular B-splines over shell surfaces, then the dynamics of thin-shell simulation is computed through the minimization of Kirchhoff-Love energy. The advantages given by our paradigm are: FEM simulation of arbitrary manifold without meshing and data conversion, and the integrated approach for geometric design and dynamic simulation/analysis. Our system also provides a level-of-detail sculpting tool to manipulate the overall shapes of thin-shell surfaces for effective design. The proposed framework has been evaluated on a set of spline models of various topologies, and the results demonstrate its efficacy in physics-based modeling, interactive shape design and finite-element simulation.

1 Introduction

Flexible plates and shells are the fundamental geometric structures found in many fields of applied engineering nowadays. Since physics-based method is of great popularity for geometric modeling and simulation in CAD/CAM, the simulation of thin-shell objects is frequently required in modern engineering design practice. However, the modeling and simulation of thin-shells have traditionally been treated as two different stages due to the lack of a common representation scheme. An intermediate data conversion process is often employed to couple the modeling and simulation, but it may deteriorate both accuracy and robustness of the whole system. Therefore, an unified representation would be ideal to overcome such difficulties.

In theory, FEM can provide an approximate solution to the problem of thin-shell deformation, but it still remains as a challenging problem due to two obstacles: Traditional finite-element is exclusively defined on planar domain, thus incapable of describe smooth surfaces and accompanying vector fields of complex manifolds and topologies

without patching/trimming; Thin-shell finite-element must be at least C^1 continuous to ensure the convergence of the solution according to Kirchhoff-Love theory. However, traditional finite-elements, endowed with purely local polynomial shape functions, usually suffer from the difficulties in enforcing the desired C^1 continuity across the element boundaries.

A number of different approaches have been attempted to combat the aforementioned obstacles in thin-shell simulation. Due to the inherent difficulties in C^1 interpolation, alternative methods have been proposed to compromise the C^1 continuity requirement, such as degenerated solid elements, reduced-integration penalty methods, and many others[1, 2]. Most recently, Cirak *et al.* [3] used the shape functions induced by subdivision rules for thin-shell finite-element simulation. Despite their modeling advantages, the subdivision surfaces do not allow close-form analytic for their basis functions, and have more unnecessary extraordinary points depending on the connectivity of the control mesh (instead of the intrinsic topology of the manifold). Another noteworthy FEM presented in [4] uses Element-Free Galerkin (EFG) method to simulate and analyze Kirchhoff shells and plates. However, it requires extra efforts to combine the model geometry with the simulation process via data conversion. In general, all these approaches fail to provide an effective way to handle thin-shell surfaces with sophisticated topology.

In this paper we articulate a novel framework that naturally couples the modeling and simulation processes for aribitrary thin-shell surfaces. Spline surfaces are prevalent in commercial modeling systems because of their unique advantages in shape modeling, manufacturing and visualization. With the recent development of manifold spline theory [5], which enables the flexible construction of splines over any manifold of arbitrary topologies, we particularly introduce a novel thin-shell finite-element based on triangular B-spline [6] defined over manifold domain. The advantages of our method over the previous state-of-the-art thin-shell simulation include: First, the shell objects of arbitrary topology can be easily modeled by manifold triangular B-splines, with a minimum number of singular points intrinsic to the topological structures of the manifolds; Second, the C^1 continuity requirement can be easily achieved for triangular B-splines; Finally, our spline-based primitive naturally integrates geometric modeling with physical simulation by avoiding unnecessary data conversion and meshing procedure, which can lead to faster product design and development cycle.

2   Spline Representation of Manifold Surfaces

In [5], Gu, He and Qin systematically build the theoretic framework of manifold spline, which locally is a traditional spline, but globally defined on the manifold. First, the manifold is covered by a special atlas, such that the transition functions are affine. Then, the knots are defined on the manifold and the evaluation of polar form is carried out on the charts. Although on different charts, the knots are different, the evaluation value is consistent and independent of the choice of charts. Furthermore, the existence of such
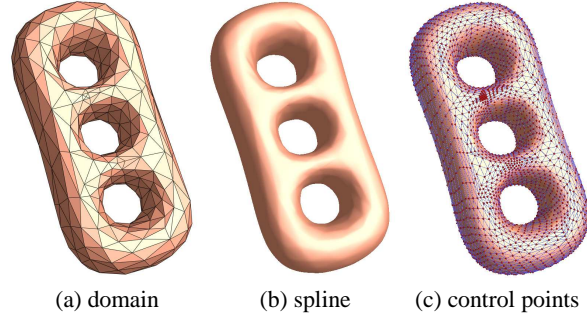
(a) domain   (b) spline   (c) control points

Fig. 1. A genus-3 manifold triangular B-spline. (a) domain manifold with 742 triangles. (b) cubic manifold triangular B-spline surface. (c) spline overlaid with control points

atlas depends on the domain topology. This new paradigm unifies traditional subdivision surfaces and splines.

The geometric intuition of the definition of manifold spline is that first we replace a planar domain by the atlas of the domain manifold, and then all the constituent spline patches naturally span across each other without any gap. The central issue of constructing manifold splines is that the atlas must satisfy some special properties in order to meet all the requirements for the evaluation independence of chart selection.

In [5], Gu et al. show that for a local spline patch, the only admissible parameterizations differ by an affine transformation. This requires that all the chart transition functions are affine. Furthermore, they show that given a domain manifold M of genus g, a manifold triangular B-spline can be constructed with no more than $|2g - 2|$ extraordinary points.

The manifold triangular B-spline can be written as follows:

$$\mathbf{F}(\mathbf{u}) = \sum_{I} \sum_{|\beta|=n} \mathbf{c}_{I,\beta} N(\phi(\mathbf{u})|V_\beta^I), \quad \mathbf{u} \in M \tag{1}$$

where $\mathbf{c}_{I,\beta} \in \mathbb{R}^3$ are the control points. Given a parameter $\mathbf{u} \in M$, the evaluation can be carried out on arbitrary charts covering $\mathbf{u}$.

Manifold triangular B-splines have many valuable properties which are critical for geometric and solid modeling. For examples, manifold triangular B-splines are piecewise polynomial defined on the manifold domain of arbitrary triangulation. Therefore, the computation of various differential properties, such as normals, curvatures, principal directions, are robust and efficient. The splines have local support, i.e., the movement of a single control point $\mathbf{c}_{I,\beta}$ only influences the surface on the triangle I and on the triangles directly surrounding I. The manifold triangular B-splines are completely inside the convex hull of the control points. The degree n manifold triangular B-splines are of C^{n-1}-continuous if there are no degenerate knots. Furthermore, by intentionally placing knots along the edges of the domain triangulation, we can model sharp features easily. The manifold spline of genus $g(\geq 1)$ has $2g - 2$ singular points. See Figure 1 for an example of genus-3 manifold triangular B-spline.

3 Spline Thin-shell Simulation

3.1 Elastic Thin-shell Mechanics

The mechanical response of a spline surface with an attached thickness property can be computed with the classical Kirchhoff-Love shell theory. In the interest of smooth technical flow, let us briefly review the derivation of thin-shell equations. Detailed presentation of classical shell theories can be found elsewhere in mechanical engineering literatures.

Thin-shell is a particular form of three-dimensional solid whose thickness is significantly small as compared with the other two dimensions. Let $\mathbf{X}(\theta_1, \theta_2)$ denote the middle surface of the thin shell, where θ_1 and θ_2 are the parametric coordinates of the surface. The generic configuration of the shell can be described as

$$S = \{\mathbf{x} \in R^3 | \mathbf{x} = \mathbf{X}(\theta_1, \theta_2) + \theta_3 \mathbf{X}_{,3}(\theta_1, \theta_2), \quad -\frac{h}{2} \leq \theta_3 \leq \frac{h}{2}\},$$

where $\mathbf{X}_{,3}$ is a unit director vector normal to the middle surface of the shell both in the reference and deformed configuration under the Kirchhoff-Love hypothesis. The internal energy of the shell depends on the differential quantities of the middle surface, such as the metric and curvature tensor. Assuming linearized kinematics, the displacement field of the middle surface is introduced as $\mathbf{u}(\theta_1, \theta_2) = \mathbf{X}(\theta_1, \theta_2) - \mathbf{X}^0(\theta_1, \theta_2)$, where the superscript "0" is used to denote the measurement in the reference configuration. Thus, the linearized membrane and bending strain tensor can be expressed as:

$$\varepsilon_{ij} = \frac{1}{2}(\mathbf{X}_{,i}^0 \cdot \mathbf{u}_{,j} + \mathbf{X}_{,j}^0 \cdot \mathbf{u}_{,i}), \tag{2}$$

$$\rho_{ij} = -\mathbf{u}_{,ij} \cdot \mathbf{X}_{,3}^0 + (\mathbf{J}^0)^{-1}[\mathbf{u}_{,1} \cdot (\mathbf{X}_{,ij}^0 \times \mathbf{X}_{,2}^0) + \mathbf{u}_{,2} \cdot (\mathbf{X}_{,1}^0 \times \mathbf{X}_{,ij}^0)]. \tag{3}$$

where $\mathbf{J} = |\mathbf{X}_{,1} \times \mathbf{X}_{,2}|$, $\mathbf{X}_{,3} = \mathbf{J}^{-1}(\mathbf{X}_{,1} \times \mathbf{X}_{,2})$, and $|\mathbf{X}_{,3}| = 1$. Here, the subscripts take the values of 1 and 2, and a comma denotes partial differentiation. Note that, the derivation of the membrane and strain is independent of the introduction of the kirchhoff-Love hypothesis.

Under the assumption of linearity of elasticity, the strain energy density is defined as follows:

$$W(\mathbf{u}) = \frac{1}{2}\frac{Eh}{1-v^2}H^{\alpha\beta\gamma\delta}\varepsilon_{\alpha\beta}\varepsilon_{\gamma\delta} + \frac{1}{2}\frac{Eh^3}{12(1-v^2)}H^{\alpha\beta\gamma\delta}\rho_{\alpha\beta}\rho_{\gamma\delta}, \tag{4}$$

in which, the first term is the membrane strain energy density and the second one is the bending strain energy density. Thus, the overall potential energy is as follow:

$$E(\mathbf{u}) = \int_\Omega W(\mathbf{u})d\Omega + E_{ext} = E_{int} + E_{ext},$$

where E_{int} is the internal elastic energy and E_{ext} is the potential of the applied forces. Following the principle of minimum potential energy, we can get the stable equilibrium

configurations of the thin-shell. The Euler-Lagrange equations corresponding to the minimum principle may be expressed in the weak form as:

$$\langle DE_{int}(\mathbf{u}), \mathbf{v} \rangle + \langle DE_{ext}(\mathbf{u}), \mathbf{v} \rangle = 0 \tag{5}$$

where $\mathbf{v}$ is the trial displacement field.

3.2 Spline Element Discretization

Following the construction of manifold triangular *B*-splines given in (1), we can extract the basis functions and write them by:

$$\varphi^l(\phi(\mathbf{v})) = \sum_{\xi(I,\beta)=l} N(\phi(\mathbf{v})|V_\beta^I) \quad \mathbf{v} \in M \tag{6}$$

in which $\xi : \mathbb{N} \times \mathbb{N}^3 \to \mathbb{N}$ associates each local simplex-spline with an unique global shape functions it contributes to, ϕ is the conformal mapping, and $\phi(\mathbf{v})$ denotes the point in the planar domain, mapped from a manifold point $\mathbf{v}$. We will use these expression in the following discussion, and represent $\phi(\mathbf{v})$ by $\mathbf{x}$ if necessary.

Thus, we can easily extend the membrane and bending strain tensors from planar parametric domain to manifold domain and write them in the form:

$$\varepsilon(\phi(\mathbf{v})) = \sum_{l=1}^{L} \mathbf{M}^l(\phi(\mathbf{v}))\mathbf{u}_l, \tag{7}$$

$$\rho(\phi(\mathbf{v})) = \sum_{l=1}^{L} \mathbf{B}^l(\phi(\mathbf{v}))\mathbf{u}_l \tag{8}$$

where $\mathbf{B}^l$ are the membrane and bending strain matrices, and $\{\mathbf{u}_l, l = 1, \ldots, L\}$ are the nodal displacement vectors.

Substituting equations (7) and (8) into (5) yields the linear equations developed from the manifold domain as:

$$\mathbf{KU} = \mathbf{F} \tag{9}$$

where $\mathbf{K}$ is the stiffness matrix, $\mathbf{U}$ is the collection of nodal displacement $[\mathbf{u}_1^T \cdots \mathbf{u}_L^T]^T$, and $\mathbf{F}$ is the nodal force vector. $\mathbf{K}$ is a block matrix which can be conveniently assembled by filling in the following 3×3 matrices:

$$\mathbf{K}^{IJ} = \int_M \left[\frac{Eh}{1-v^2}(\mathbf{M}^I)^T \mathbf{H} \mathbf{M}^J + \frac{Eh^3}{12(1-v^2)}(\mathbf{M}^I)^T \mathbf{H} \mathbf{M}^J \right] dM$$

with the constitutive matrix $\mathbf{H}$ made of contravariant metric tensors, the definition of which is available in [3]. The construction of $\mathbf{F}$ will be discussed later.

3.3 Implementation Details

Numerical Integration: The thin-shell FEM simulation needs to compute the Kirch-hoff energy of the deformed shell surfaces. However, the evaluation of the integrations over arbitrary manifold surfaces has been a challenging problem, which is usually awkwardly handled by piecewise parameterizations. With the global conformal mapping coupled with triangular *B*-splines theory, we can conduct the integration on an equivalent planar domain instead, and use any established numerical integration techniques. In our system, the shell elements are selected as the triangles of the tessellation, from which the triangular spline is constructed. Then we regularly subdivide each element into small congruent triangles, and compute the integration using triangle Gaussian quadratures.

Boundary Condition Handling: To facilitate the process of intuitive geometric design, we include point-based constraints as the input for our thin-shell simulation system. The users are allowed to pick up a group of points on the spline surfaces, i.e. $\mathbf{P}^0 = \{p_1^0, p_2^0, \ldots, p_n^0\}$, and assign them with desired positions after the deformation, i.e. $\mathbf{P} = \{p_1, p_2, \ldots, p_n\}$, where n denotes the total number of the point constraints. This linear constraints thus defined can be grouped in a matrix format as:

$$\mathbf{P}^0 + \mathbf{C}\mathbf{u} = \mathbf{P}$$

where $\mathbf{C}$ is an extremely sparse matrix that stores the basis function values at corresponding constraint points $\mathbf{P}^0$. To combine the constraints with the Equation (9), we solve for $\mathbf{u}$ in the Null-space of $\mathbf{C}$, such that:

$$\mathbf{u} = \mathbf{N}\mathbf{u}' + \mathbf{u}^0$$

where $\mathbf{C}\mathbf{N} = 0$ and $\mathbf{C}\mathbf{u}^0 = \mathbf{P} - \mathbf{P}^0$. We use gaussian-jordan-elimination-like approach[7] to construct $\mathbf{N}$, and solve for $\mathbf{u}^0$ by either singular value decomposition (SVD) or QR decomposition method. Due to the extreme sparsity and rank-deficiency of $\mathbf{C}$, such method is computationally viable to handle point-based geometric constraints.

Level-of-Detail (LOD) Simulation: The shell objects with affluent surface details requires massive number of degrees of freedom (DOF) for accurate geometric modeling. However, the triangular *B*-splines models having large number of control points are not suitable for interactive geometric design. Thus, we incorporate a level-of-detail (LOD) strategy to accommodate thin-shell deformation of sophisticated models. Any thin-shell surfaces $\mathscr{S}$ can be decomposed to a smooth spline-based surface $\mathbf{S}_0$ and a scalar function d describing the additional displacements, i.e.:

$$\mathbf{S}(\mathbf{x}) = \mathbf{S}_0(\mathbf{x}) + d(\mathbf{x}) \cdot \mathbf{n}(\mathbf{x})$$

where $\mathbf{n}$ is the normal vector of $\mathbf{S}_0$. Practically, $\mathbf{S}_0$ can be estimated by fitting the original surface using manifold triangular *B*-spline with relatively small number of control points [8]. Then the magnitudes of the fitting errors along the normal directions will be further modeled as a spline-based function d with more degree of freedoms. For the LOD simulation of a complicated thin-shell model, our system allows users to sculpt on

the base surfaces $\mathbf{S}_0$, then the previously recorded details will be automatically applied to give the final design results. Figure.2 gives two examples of geometric design with LOD thin-shell simulation.

4 Results

Our system is implemented on a Microsoft Windows XP PC with Intel Pentium IV 3.0GHz CPU, 1.0GB RAM, and an nVidia GeForce Fx 5600 Ultra GPU. We have run a variety of examples to verify and test the efficacy and performance of our method. These examples includes a female face, the stanford bunny, a torus and a kitty. Both the face and the bunny are LOD-modeled. And both the torus and the kitty models have non-trivial genus.
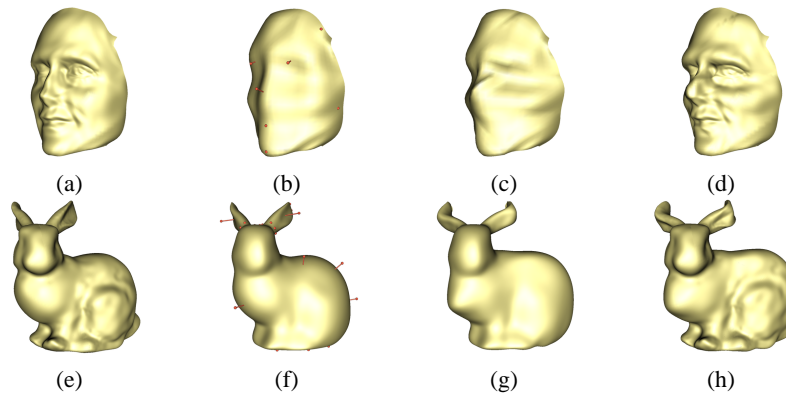

(a)	(b)	(c)	(d)
(e)	(f)	(g)	(h)

Fig. 2. LOD thin-shell simulation (a)(e) the original surfaces with feature details. (b)(f) the base surfaces with geometric constraints. (c)(g) the base surfaces after thin-shell deformation. (d)(h) the original surface after LOD thin-shell deformation.

5 Conclusion

In this paper, we propose a novel paradigm that successfully simulates the elastic deformation of thin-shell objects. We also provide users with a LOD sculpting tool for esthetical geometric design. The experiment results show demonstrate that the proposed thin-shell FEM method has the following advantages over the traditional ones. It can easily achieve the C^1 continuity requirement, and represent arbitrary thin-shell surfaces using splines with minimum number of singular points. Our spline-based primitive naturally integrates geometric modeling with physical simulation in the entire CAD/CAM process, thus unnecessary data conversion and meshing procedure is total avoided. For
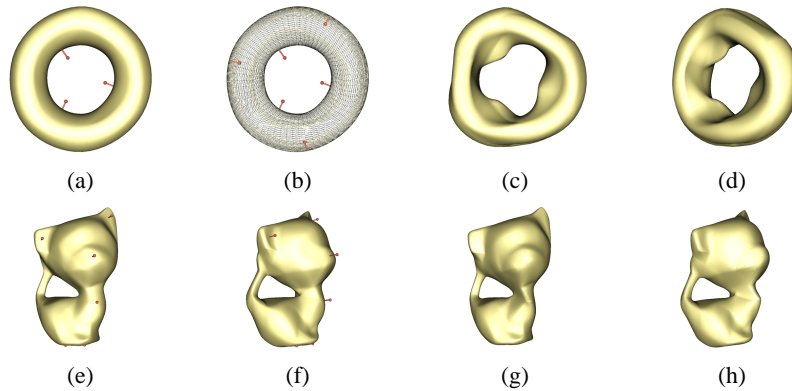
Fig. 3. (a)(b) 6 points constraints applied on the torus surface. (c)(d) torus shell after deformation. (e)(f) the front and side view of the kitty with points constraints. (g)(h) the front and side view of the deformed kitty shell.

future work, we will extend current framework to handling large thin-shell deformation by considering non-linear elastic energy, and solve the simulation problem in temporal dimension for animation applications.

Acknowledgements

References

1. Bucalem, M., Bathe, K.: Finite element analysis of shell structures. Arch. Comput. Method Eng. **4** (1997) 3–61
2. MacNeal, R.: Perspective on finite elements for shell analysis. Finite Elem. Anal. Des. **30** (1998) 175–186
3. Cirak, F., Ortiz, M., Schröder, P.: Subdivision surfaces: a new paradigm for thin-shell finite element analysis. Int. J. Numer. Methods Eng. **47** (2000) 2039–2072
4. Krysl, P., Belytschko, T.: Analysis of thin plates by the element-free galerkin method. Comput. Mech. **17** (1996) 26–35
5. Gu, X., He, Y., Qin, H.: Manifold splines. In: Proc. ACM Symp. Solid and Physical Modeling. (2005) 27–38
6. Dahmen, W., Micchelli, C.A., Seidel, H.P.: Blossoming begets b-spline built better by b-patches. Math. Comput. **59**(199) (1992) 97–115
7. Celniker, G., Welch, W.: Linear constraints for deformable non-uniform b-spline surfaces. In: Proc. ACM Symp. Interactive 3D Graphics. (1992) 165–170
8. He, Y., Qin, H.: Surface reconstruction with triangular b-splines. In: Proc. Geometric Modeling and Processing. (2004) 279–290